Delocalization of classical waves in highly anisotropic random media

Alex Small[1,*] and David Pine[2]

[1]*Laboratory of Integrative and Medical Biophysics, National Institute of Child Health and Human Development,*
National Institutes of Health, Bethesda, Maryland 20892, USA
[2]*Department of Physics, New York University, New York, New York 10003, USA*

We discuss localization phenomena in multilayer films doped with scattering particles. If the films exhibit a particular type of transmission resonance then above a critical frequency waves in the sample can decay as a power law rather than exponentially. This phenomenon is independent of the scattering strength of the particles, in stark contrast to previous work. We find that this phenomenon has many similarities to a second order phase transition. This work points to interesting avenues in the study of waves in anisotropic disordered media.

PACS number(s): 42.25.Dd, 42.25.Bs, 05.40.−a

I. INTRODUCTION

Recent interest in localization of classical waves [1–4] has been driven by advances in the processing of materials with structure on length scales comparable to the wavelength of light, including photonic crystals [3,5]. Advances in materials synthesis and processing have also expanded the tool kit of engineered materials to include photonic materials with highly directional or anisotropic properties. Effects such as anisotropic diffusion [6] and anisotropic coherent back-scattering have been observed [7]. The new possibilities opening up in the study of anisotropic photonic materials motivate us to seek previously unexplored phenomena in the theory of wave propagation in anisotropic media.

Theoretical studies of anisotropic materials have focused on layered media with dopants that break the translational symmetry perpendicular to the layering direction [8–10]. Earth's layered crust is one obvious example of such a medium, the understanding of which is relevant to seismology, geology, and oil exploration. Sheng and co-workers examined such systems in a series of papers beginning fifteen years ago. They considered the Anderson model with disorder that could be "tuned" from isotropic (e.g., powders, or amorphous electronic materials) to strongly anisotropic (layered structure). One of the key findings was that above a critical degree of anisotropy the transport along the layering direction was dominated by one-dimensional (1D) localization, despite the presence of dopants that break translational symmetry transverse to the layering direction [8]. Transport in the axial direction was found to be localized when the system is strongly anisotropic, but transport in the transverse direction was found to be diffusive.

However, previous studies of waves in anisotropic media have largely ignored the influence of phenomena that can lead to anomalously high transmission. In 1D disordered media, all solutions of the wave equation are localized, with the possible exception of a set of freely propagating states at discrete frequencies [11]. These discrete frequencies correspond to perfect or near-perfect transmission, and are often referred to as transmission resonances.

Anomalously large transmission of classical waves through 1D (as opposed to anisotropic 3D) disordered systems has been studied primarily in two contexts. The first (and most common) situation is transmission resonances that arise from constructive interference of forward-scattered waves and destructive interference of reflected waves [12]. These sharp resonances can occur in a wide range of systems and are a subject of active interest [13]. They are characterized by narrow resonances at discrete angles and frequencies, with widths that decreases exponentially with sample thickness.

The second type of anomalous transport in a 1D disordered system is referred to as a "Brewster anomaly," and results when light propagates through a disordered multilayer medium at or near the Brewster angle [14,15]. The two polarization components decouple in such media, and for one of the polarizations the localization length ξ diverges at the Brewster angle, as the slabs do not back-scatter waves incident with a particular angle and polarization. The signature of this phenomenon is that ξ depends on angle but not on frequency. However, this phenomenon is limited to electromagnetic waves.

In this work, we study another type of resonance that is particularly simple but is not limited to electromagnetic waves. We consider anisotropic media with transmission resonances resulting from Fabry-Perot resonances of the individual scatterers [16]. We study classical scalar waves for simplicity, but the underlying phenomenon holds for electromagnetic and other types of waves. There are a few close analogies between our work and Brewster anomalies, but the phenomenon that we study is frequency dependent, which leads to unique effects.

We will show that Fabry-Perot transmission resonances can lead to incredibly rich behavior in a seemingly simple system. We predict delocalization of waves above a critical frequency equal to the frequency of the first Fabry-Perot resonance (aside from a possible trivial resonance at zero frequency). The delocalized states are not propagating states, as they undergo power law decay along the layering direction, but they decay more slowly than exponentially localized states. The delocalization transition is in many ways analogous to a second order phase transition. These previously unanticipated phenomena raise the possibility that

---

*Electronic address: smallalex@mail.nih.gov
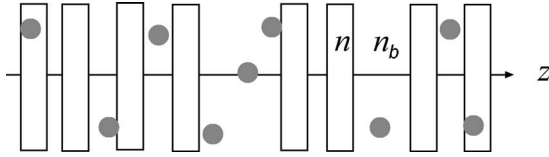
FIG. 1. Sketch of the anisotropic medium under consideration, consisting of identical slabs of refractive index n aligned along the z axis in a medium of refractive index n_b and doped with particles (circles).

waves in anisotropic disordered media may exhibit much richer behavior than previous studies have anticipated.

II. OUR MODEL SYSTEM

The system under study is a material composed of a series of identical dielectric slabs with thickness d and refractive index n, all aligned perpendicular to the z axis. (Fig. 1) They are separated from one another by random intervals, and they are surrounded by a medium of refractive index n_b. Well-studied examples of such a system include Thue-Morse [17] and Fibonacci [18] multilayer films. The medium is doped with small particles that scatter weakly.

III. RESONANCES OF SINGLE SLABS AND MULTILAYER STACKS

A. Scattering from single slabs

We begin our analysis by considering resonant transmission through a single slab. The reflectance (at normal incidence) of a single slab surrounded by a medium of refractive index n is given by [16]

$$R = \frac{4r^2 \sin^2 k_{z2}d}{(1-r^2)^2 + 4r^2 \sin^2 k_{z2}d}, \qquad (1)$$

where

$$r = \frac{k_{z1} - k_{z2}}{k_{z2} + k_{z1}}, \qquad (2)$$

$k_{z2} = nk_0$, $k_{z1} = n_b k_0$, $\omega = ck_0$ is the frequency of the wave incident on the slab, and c and k_0 are, respectively, the speed of light in vacuum and the wave number of the wave in vacuum. At frequencies that are integer multiples of a critical frequency $\omega_c = \pi c/nd$, the reflectance at normal incidence is zero due to destructive interference.

Now, consider the case where a wave is incident on a slab from off-normal incidence. We will not describe the incident direction by its angle with respect to the z axis or by the z component of the **k** vector, because these variables change due to refraction when passing from the surrounding medium to the slab. Instead, we will describe the incident wave by $\mathbf{k}_t$, the transverse portion of the wave vector, which is unchanged by reflection and refraction in a multilayer medium and is hence a position-independent variable to describe the wave. In this case, the reflectance of the slab is given again by Eq. (1), with the following modifications [16]:

$$k_{z2} = \sqrt{n^2 k_0^2 - k_t^2}, \quad k_{z1} = \sqrt{n_b^2 k_0^2 - k_t^2}. \qquad (3)$$

The slab's azimuthal symmetry leads to R depending only on k_t, the magnitude of $\mathbf{k}_t$.

The reflectance is zero when

$$\sqrt{n^2 k_0^2 - k_t^2} = m\frac{\pi}{d}, \qquad (4)$$

where m is an integer. When Eq. (4) is satisfied a wave undergoes an integer number of half cycles of oscillation while traversing the slab. Once again, destructive interference between the wave reflected from the surface of the slab and the wave reflected internally leads to resonant transmission. If we vary k_0 and $\mathbf{k}_t$ (i.e., vary the frequency as well as the direction of propagation), resonant transmission through the slab is possible over a range of frequencies above ω_c, with a different direction of propagation for each frequency. We note that, although this condition was derived for classical scalar waves, Eq. (4) holds for electromagnetic waves incident on a slab, irrespective of polarization.

B. Theory of multilayer stacks

Next consider what happens in a stack of parallel slabs with identical thicknesses d but random spacing. Because reflection and refraction by the slabs do not change $\mathbf{k}_t$, states with different transverse wave vectors are uncoupled, and we can catalog the possible channels for waves to scatter into by their frequencies and transverse wave vectors. For a given frequency, waves incident in all directions will be attenuated except over a cone of angles corresponding to the Fabry-Perot resonances of the slabs [see Eq. (4)].

In general, the phenomenon of localization in one dimension will cause exponential attenuation of waves transmitted through our sample. However, when the identical slabs are either transparent or reflect only weakly (i.e., for directions at or near a Fabry-Perot resonance in our system), the mean free path for scattering can be comparable to or larger than the system size. Localization requires significant scattering and destructive interference of forward-scattered waves, and the exponential decay characteristic of localized waves is normally a statistical feature of wave behavior that is only evident over long distances. It is therefore not conceptually satisfying to apply the term "localized" to waves propagating through our system at or near a Fabry-Perot resonance. Nonetheless, when energy is distributed over a range of angles inside such a multilayer stack, transmission will be dominated by waves in resonant and near-resonant channels (directions of propagation). We will therefore formulate an appropriate theoretical description of transmission via resonant or near-resonant channels.

We can calculate the mean free path ℓ from the relation

$$\ell^{-1}(\omega, k_t) = R(\omega, k_t)\rho_s, \qquad (5)$$

where $R(\omega, k_t)$ is the reflectance of a slab for a given frequency and transverse wave vector, and ρ_s is the number density of slabs per unit length. If we expand Eq. (1) as a function of k_t in the vicinity of a value of k_t satisfying the

resonance condition Eq. (4) (we shall call this $k_{t,res}$), after much algebra we get that (to lowest order in $|k_t - k_{t,res}|$)

$$\ell^{-1}(\omega, k_t) \approx \beta \rho_s |k_t - k_{t,res}|^2 k_{t,res}^2 d^4, \qquad (6)$$

where β is a dimensionless factor of order 1, determined by the values of $n_b k_0 d$ and $k_{t,res} d$. For resonant transmission ℓ^{-1} is zero, corresponding to an infinite mean free path.

In order to model transport over long distances inside a multilayer stack, we need to know the localization length $\xi(\omega, k_t)$ for waves with a given frequency and transverse wave vector, since the intensity of light transmitted through a multilayer stack decays (on average) as

$$T = e^{-2L/\xi(\omega, k_t)}, \qquad (7)$$

where L is the sample thickness. In general, $\xi(\omega, k_t)$ depends on the detailed configuration of a system, since the transmitted field is governed by interference between multiply scattered waves. However, if we consider an ensemble of systems with the same total size and same number density of slabs per unit length, and vary the spacing between the slabs, we can use the ensemble-averaged transmittance to calculate an average localization length from Eq. (7). In the limit of a large ensemble, the localization length $\xi(\omega, k_t)$ is proportional to $\ell(\omega, k_t)$ by a factor of order ≈ 4 [11].

We therefore conclude that, for waves propagating in directions near to a Fabry-Perot resonance, the localization length $\xi(\omega, k_t)$ will scale as

$$\xi^{-1}(\omega, k_t) = \gamma \rho_s |k_t - k_{t,res}|^2 k_{t,res}^2 d^4, \qquad (8)$$

where $\gamma \approx 4\beta$ is a dimensionless number of order unity.

Our results for the scaling of the ensemble-averaged localization length are verified with numerical simulations in the Appendix.

IV. MULTILAYER STACKS DOPED WITH PARTICLES

We now consider what happens when we dope our systems with small scattering particles. For simplicity we assume that the particles are spherical and identical, but we can also assume that they are nonspherical but randomly oriented. If we illuminate the system with a monochromatic plane wave incident parallel to the z axis at $z=0$, the incident wave will couple to a localized state with $k_t=0$. The effect of the particles will be to scatter a portion of the energy into other localized states with different transverse wave vectors. We will assume that the (ensemble averaged) intensity profiles of the localized states decay as $e^{-2z/\xi}$.

The field $\phi(\mathbf{r})$ inside the multilayer stack can be written as a superposition of modes with different transverse wave vectors $\mathbf{k}_t$:

$$\phi(\mathbf{r}) = \int a(\mathbf{k}_t) \phi(\mathbf{k}_t, \mathbf{r}) e^{i\mathbf{k}_t \cdot \mathbf{r}} d^2 \mathbf{k}_t, \qquad (9)$$

where $\phi(\mathbf{k}_t, \mathbf{r})$ is the field amplitude at a position $\mathbf{r}$ inside the sample for a mode with transverse wave vector $\mathbf{k}_{t1}$, and $a(\mathbf{k}_t)$ gives the projection of the field onto that mode. We assume that, when averaged over an ensemble of similar systems, the

intensity $|\phi(\mathbf{k}_{t1}, \mathbf{r}_j)|^2$ decays exponentially as $e^{-2z/\xi(\omega, k_t)}$, where $\xi(\omega, k_t)$ is given by Eq. (8). The square of the projection, $|a(\mathbf{k}_t)|^2$ depends only on the magnitude of the transverse wave vector due to the fact that there is no preferred azimuthal direction in the system, so we can write $|a(\mathbf{k}_t)|^2 = |a(k_t)|^2$.

We want to calculate the ensemble-averaged intensity inside the system as a function of distance z along the axis. We are interested in the intensity averaged over the cross-sectional area of the sample (i.e., averaged over the xy plane), and so we can use Parseval's Theorem to convert an integral over the cross sectional area to an integral over all possible transverse wave vectors $\mathbf{k}_t$:

$$I(z) \propto \int |\phi(\mathbf{r})|^2 dx dy \propto \int_0^{k_{t,max}} |a(k_t)|^2 e^{-2z/\xi(\omega, k_t)} k_t dk_t, \qquad (10)$$

$k_{t,max}$ is whatever the maximum possible value of k_t is in our system. Although this integral is an incoherent addition of intensities, none of the interference effects crucial to localization are lost because it is an incoherent addition of waves traveling in different transverse directions. The exponential scaling of the localized waves accounts for 1D localization effects.

In general, for large z the integral in Eq. (10) is dominated by propagation along whichever direction corresponds to the longest localization length. If we illuminate the system with a wave of frequency $\omega < \omega_c$, the weakest reflectance (and hence the longest localization length) is obtained at normal incidence, so deep inside the sample the field will be dominated by a state localized along the z axis with $k_t=0$.

Things become more interesting for $\omega > \omega_c$. The particles will scatter part of the wave's energy into states with resonant or near resonant transmission through the slabs. These states have an unbounded continuum of localization lengths, and so there is no intrinsic length scale governing the wave's behavior deep inside the sample. For any arbitrarily large distance z inside the sample there is a continuum of states with localization lengths longer than z. We can show that in this case the wave exhibits power law behavior if we assume that in the vicinity of $k_t \approx k_{t,res}$, $|a(k_t)|^2$ is a continuous and differentiable (i.e., well-behaved) function and is not identically zero. A very general form for $|a(k_t)|^2$ in the vicinity of $k_{t,res}$ is then

$$|a(k_t)|^2 = |k_t - k_{t,res}|^{2\alpha} g(k_t - k_{t,res}), \qquad (11)$$

where $g(k_t - k_{t,res})$ is analytic, $g(0)$ is nonzero, and the value of $\alpha \geq 0$ will be determined later. For large z, the integral in Eq. (10) is dominated by contributions from resonant and near-resonant transmission, provided that the field has nonzero projection onto those states. We expand Eq. (10) to lowest order in $|k_t - k_{t,res}|$ by substituting the form for ξ^{-1} given in Eq. (8) and expanding the form for $|a(k_t)|^2$ given in Eq. (11):

$$I(z) \propto \int_0^{k_{t,max}} e^{-2\rho_s z \gamma |\Delta k_t|^2 k_{t,res}^2 d^4} |\Delta k_t|^{2\alpha}$$

$$\times [g(0) + \Delta k_t g'(0) + \mathcal{O}((\Delta k_t)^2)][k_{t,res} + \Delta k_t] d\Delta k_t, \tag{12}$$

where $\Delta k_t \equiv k_t - k_{t,res}$

We can cast the integral in Eq. (12) in terms of the dimensionless variable $u \equiv \sqrt{\gamma \rho_s z} |k_t - k_{t,res}| k_{t,res} d^2$:

$$I(z) \propto \frac{1}{(z\rho_s)^{1/2+\alpha}} \int_{u_{min}}^{u_{max}} e^{-2\gamma u^2} u^{2\alpha}$$

$$\times \left(g(0) + \frac{u}{\sqrt{\gamma \rho_s z}} \frac{g(0) + g'(0)k_{t,res}}{k_{t,res}^2 d^2} \right) du, \tag{13}$$

where $u_{min} = -\sqrt{\gamma \rho_s z} k_{t,res}^2 d^2$, and $u_{max} = \sqrt{\gamma \rho_s z} k_{t,res}(k_{t,max} - k_{t,res})d^2$.

This integral requires careful treatment. For nonzero $k_{t,res}$ (or, equivalently, $\omega > \omega_c$) and z sufficiently large, we can approximate the limits of integration as $\pm\infty$. The second term integrates to zero and the integral is a constant, leading to the scaling relationship

$$I(z) \propto z^{-(1/2+\alpha)}. \tag{14}$$

We thus find that the wave is no longer localized, with the transmission decaying as a power law instead of an exponential.

At this point, it is worth noting that the integral in Eq. (13) is dominated by contributions in the range $-1 \leq u \leq 1$. Since $u = \sqrt{\gamma \rho_s z} |k_t - k_{t,res}| k_{t,res} d^2$, this implies that most of the transmitted intensity comes from propagation in directions specified by the condition

$$|k_t - k_{t,res}| \equiv \delta k_t \leq \frac{1}{\sqrt{\gamma \rho_s z} k_{t,res} d^2}. \tag{15}$$

This condition defines a cone of angles with finite width δk_t. Transport through directions within the cone implies transport in a state with localization length $\xi(\omega, k_t) \gtrsim z$, which is what we would expect physically.

For ω sufficiently close to ω_c, the integral in Eq. (13) requires a more careful treatment. The limits of integration in Eq. (13) are asymmetric. As long as the limits of integration extend outside the range where e^{-2u^2} is of order unity the second term in Eq. (13) integrates to zero. However, when $\sqrt{\rho_s z}(k_{t,res} d)^2$ is of order unity or smaller, the second term no longer integrates to zero, and its magnitude is no longer negligible relative to the first term. It is easy to show that the second term in Eq. (13) decays exponentially both as a function of z and as a function of $|\omega - \omega_c|$, and so the second term in Eq. (13) produces a localized wave with an amplitude that is negligible except at frequencies near ω_c.

Before we try to predict the value of α, it is easy to see that α must be at least $\frac{1}{2}$. If there were no slabs in the system, or if the slabs were index-matched to the background medium ($n = n_b$), wave transport would be diffusive and the intensity inside the medium would decay as z^{-1}. Introducing the slabs should obviously further attenuate wave propagation in the system, and so above the critical frequency the wave should decay at least as rapidly as z^{-1}. (In principle, of course, slabs could enhance transmission due to interference effects for a particular configuration. However, in the ensemble-averaged case that we consider here, the effect of introducing slabs will be to reduce the ensemble-averaged transmission.)

V. DETERMINING THE EXPONENT

To calculate α we invoke the principle of detailed balance to determine the distribution of energy among the various modes. The instantaneous rate at which a single particle j scatters energy from a mode $(\mathbf{k}_{t1}, \omega)$ to a mode $(\mathbf{k}_{t2}, \omega)$ is

$$|a(\mathbf{k}_{t1})|^2 |f_j(\mathbf{k}_{t1}, \mathbf{k}_{t2})|^2 |\phi(\mathbf{k}_{t1}, \mathbf{r}_j)|^2, \tag{16}$$

where $f_j(\mathbf{k}_{t1}, \mathbf{k}_{t2})$ is proportional to the form factor for particle j to scatter light from a mode with transverse wave vector $\mathbf{k}_{t1}$ to a mode with transverse wave vector $\mathbf{k}_{t2}$. The total instantaneous rate $R_{1 \to 2}$ of scattering from a mode $(\mathbf{k}_{t1}, \omega)$ to a mode $(\mathbf{k}_{t2}, \omega)$ is therefore

$$R_{1 \to 2} = |a(|\mathbf{k}_{t1}|)|^2 |f(\mathbf{k}_{t1}, \mathbf{k}_{t2})|^2 \sum_{particles\ j} |\phi(\mathbf{k}_{t1}, \mathbf{r}_j)|^2. \tag{17}$$

Our assumption that the particles are identical and spherical (or at least randomly oriented) enables us to bring the scattering amplitude f outside the summation and remove the subscript j. Equation (17) accounts for all multiple scattering effects from the particles. The summation itself depends only on the state being scattered out of, is inversely proportional to the lifetime of the state $(\mathbf{k}_{t1}, \omega)$, and will henceforth be denoted $\tau^{-1}(\mathbf{k}_{t1})$. Being a sum over particles, the inverse lifetime is just proportional to the number of particles probed by that state, and hence the spatial extent of the state. The natural measure of the spatial extent of a state is the localization length. We therefore have that

$$\tau^{-1}(\mathbf{k}_t) \propto \xi(\mathbf{k}_t) \propto |k_t - k_{t,res}|^{-2}. \tag{18}$$

To obtain information on $|a(|\mathbf{k}_{t1}|)|^2$ we impose the steady state condition. In a steady state the rate of scattering from a state 1 to a state 2 should be equal to the rate of scattering from state 2 to state 1. Our task is simplified by the fact that, due to time-reversal symmetry, $|f(\mathbf{k}_{t1}, \mathbf{k}_{t2})|^2 = |f(\mathbf{k}_{t2}, \mathbf{k}_{t1})|^2$, and hence the form factor cancels out. Since the rate of scattering from 1 to 2 is equal to $\tau^{-1}(1)$ and the rate of scattering from 2 to 1 is equal to $\tau^{-1}(2)$, in steady state the ratio $|a(|\mathbf{k}_{t1}|)|^2 / |a(|\mathbf{k}_{t2}|)|^2$ is $\tau(\mathbf{k}_{t1})/\tau(\mathbf{k}_{t2})$, so

$$|a(k_t)|^2 \propto |k_t - k_{t,res}|^2 \tag{19}$$

This analysis therefore predicts that $\alpha = 1$, and that in the multiple scattering regime the intensity will scale as $z^{-3/2}$.

It may seem strange that the projection of the field onto a resonant state is zero. However, we never normalized our basis of localized states, and so the energy stored in a state with transverse wave vector $\mathbf{k}_t$ is proportional to the localization length. The energy density is obtained by multiplying $|a(\mathbf{k}_t)|^2$ by the localization length $\xi(\mathbf{k}_t)$. Since $|a(k_t)|^2 \propto \xi^{-1}(\mathbf{k}_t)$, the energy density per state is therefore a constant.
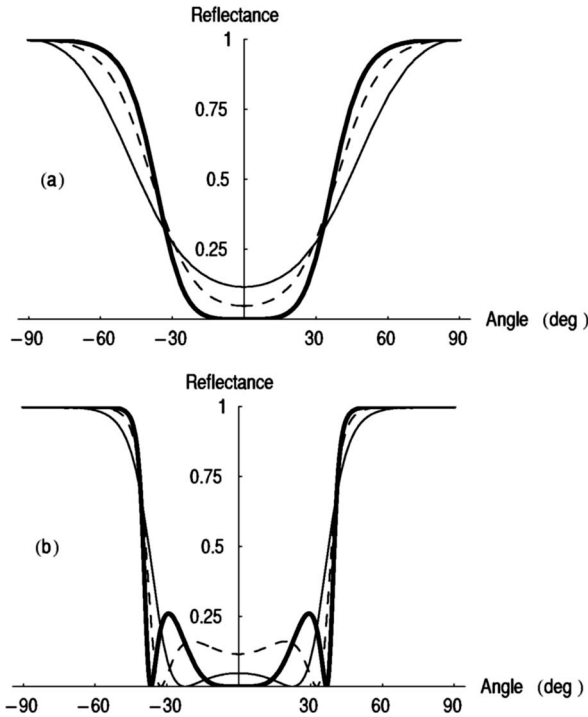
FIG. 2. Reflectance vs angle of incidence for a low index slab ($n=1$) embedded in a high index medium ($n=1.45$) at various frequencies. (a) The approach to the first transmission resonance, with $\omega=0.6\omega_c$ (thin solid line), $0.8\omega_c$ (dashed), and ω_c (thick solid line). (b) The approach to the second transmission resonance, with $\omega=1.2\omega_c$ (thin solid line), $1.6\omega_c$ (dashed), and $2\omega_c$ (thick solid line).

This is exactly what one would expect for diffusive waves.

It is interesting to note that a very crude scaling argument could have given the same result: Within the range of directions specified by Eq. (15), the slabs scatter only weakly. Transport is largely diffusive and dominated by scattering from the particles. The width of this resonance scales as $z^{-1/2}$, and the intensity of the diffusely transmitted wave scales as z^{-1}. Multiplying the diffuse transmission by the angular width of the resonance gives a diffusely transmitted intensity of $z^{-3/2}$.

VI. ANALOGY WITH MEAN FIELD THEORY AND PHASE TRANSITIONS

We can obtain further insight into the delocalization phenomenon if we examine the reflectance of a single slab versus angle of incidence. (For ease of interpretation we revert to characterizing states by angle of incidence rather than transverse wave vector.) In Fig. 2 we plot the reflectance versus angle of incidence onto an air gap ($n=1$) of thickness d surrounded by silica ($n=1.45$) and excited and probed at various frequencies. For frequencies below ω_c the reflectance minimum is at normal incidence, and the curve of reflectance versus angle shifts downward at increasing frequencies. The channel with the longest localization length is therefore the one with $k_t=0$, and the localization length decreases with increasing frequency.
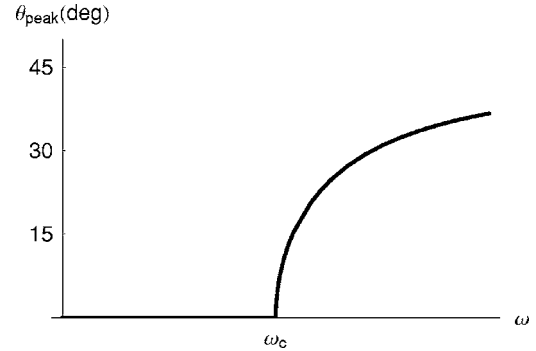
FIG. 3. The dominant direction at which transmitted waves exit the sample as a function of frequency (schematic).

At $\omega=\omega_c$, the reflectance is exactly zero at normal incidence, and above ω_c the zeroes of reflectance shift out to larger angles. Waves scattered at or near those angles by the particles will have long localization lengths and travel far into the sample, and if we were to measure the angular profile of transmitted radiation exiting the sample we would find that the peak angle would be the one that minimizes the reflectance of an individual slab.

When we consider the frequency dependence of the angular profile, it is clear that for frequencies below ω_c the intensity profile of the transmitted light will be peaked at $\theta_{peak}=0$. We illustrate this behavior (schematically) in Fig. 3. However, at frequencies above ω_c the angular profile of the transmitted light will be circular, with a peak at whichever angle minimizes the reflectance of an individual slab. Moreover, the value of θ_{peak} will be a continuously increasing function of ω. We observe that this finding is independent of our finding of delocalized power-law transport: Even if waves remained localized for $\omega>\omega_c$, transport over long distances would be strongest in those directions for which reflection from the slabs is minimized.

The behavior of θ_{peak} bears a striking resemblance to an order parameter in a system undergoing a second order phase transition. It is an easily measured macroscopic quantity with a clear geometrical significance, and it increases continuously from zero when a characteristic energy scale (frequency) is exceeded. Below that characteristic energy scale it is identically zero. We also note that the behavior of the minima in Fig. 2 bears a striking resemblance to plots of free energy versus order parameter in the mean field theory of a system undergoing a second order phase transition. Perhaps the most obvious difference between our delocalization transition and a second order phase transition is the absence of symmetry breaking. Because waves traveling in different directions cannot interact with one another there is no driving force that would break symmetry. One might, however, speculate on possibilities for symmetry breaking in nonlinear media.

VII. EXPERIMENTAL CONSIDERATIONS

A. Particle concentration

We now consider how the phenomena described thus far would manifest in an actual experiment. We begin with the

effect of varying particle concentration in actual experiments. For these purposes, imagine an ensemble of identical multilayer dielectric films that differ only in the concentration and placement of particles.

A film without particles would look like a mirror at normal incidence and angles far away from a resonance. At an angle corresponding to a resonance it would look at least somewhat transparent, although the degree of transparency might be small due to the narrow width of the resonance.

The next simplest situation would be to incorporate particles at or near the surface of the sample, or to roughen the surface by scratching or etching it. The effect would be to distribute incident light over a range of angles, including resonant and near-resonant directions. More light would be diffusely transmitted through the sample as a result, in stark contradiction to the usual effect of roughening a surface.

Finally, consider a film with particles distributed throughout its volume. If the system is illuminated by a plane wave incident at a nonresonant angle, the light will only penetrate a distance ξ_0 into the system before being reflected, where ξ_0 is the localization length of the state that the incident light couples to. At low particle concentrations, the amount of light scattered out of the incident beam by the particles will scale as $\xi_0 \rho_p \sigma$, where ρ_p is the number density of particles per unit volume and σ is the scattering cross section of a single particle. This condition remains valid as long as $\xi_0 \rho_p \sigma \lesssim 1$. The light scattered out of the incident beam by the particles is the light that will participate in the phenomena described here, and so we predict that, at low particle concentrations, the diffusely transmitted light will be proportional to particle concentration. This is very different from the usual result for diffusion of light, where transmittance is inversely proportional to scatterer concentration.

B. Angular distribution of transmitted light

As discussed above, when $\omega > \omega_c$, the angular distribution of transmitted light will have a sharp peak at whichever angle corresponds to a Fabry-Perot resonance. Suppose that we measure the angular profile of the transmitted light. The strongest signal will occur around a ring with a radius corresponding to the angle of the Fabry-Perot resonance.

The total amount of light contained in that ring is proportional to the angular cross section of the ring. The diameter of the ring scales as $k_{t,res}$, and the thickness of the ring scales as δk_t from Eq. (15). If we normalize the angular cross section by $1/k_0^2$ to obtain a measure of the solid angle, we see that the amount of light in the ring scales as $(k_0 d)^{-2}(L \rho_s \gamma)^{-1/2}$. Outside this ring, the intensity is decreasing exponentially with sample thickness, providing a sharp contrast between the bright ring and the surrounding background. We are therefore confident that the amount of light transmitted by the mechanisms considered here is significant compared with the exponentially attenuated light transported through states with short localization lengths.

In the limit of large systems, of course, transmission measurements would not be feasible due to the decay of the signal, and in the limit of a truly infinite system transmission would be a meaningless concept. However, if one has the ability to probe the local field inside the system then an ensemble-averaged intensity profile could still be measured, and the power law decay would distinguish delocalized waves from localized (exponentially decaying) waves.

C. Polydisperse slabs

Our results assume that the system contains dielectric slabs of identical thickness. In any realistic experiment, of course, the slabs will have variable thicknesses. In that case, there will be no direction of propagation for which all slabs are transparent. However, if the distribution of slab sizes is sufficiently narrow then most of the slabs will be either transparent or almost transparent to waves propagating at a certain critical angle. This critical angle is determined by the condition

$$k_{z2}\langle d \rangle = \sqrt{n^2 k_0^2 - k_{t,res}^2}\langle d \rangle = m\pi, \qquad (20)$$

where $\langle d \rangle$ is the average slab thickness and m is an integer representing the order of the resonance. Although waves propagating in or near this resonant direction will still be localized, the localization length will be very long and peaked for states at or near that direction. The output radiation will therefore exhibit the directional behavior discussed above, as long as the distribution of slab thicknesses is sufficiently narrow.

Strong transmission will be possible for the direction specified by Eq. (20) as long as the distribution of slab thicknesses is sufficiently narrow that $k_{z2} \delta d \ll \pi/2$, where δd is the standard deviation of the distribution. This condition implies that in order to observe the predicted phenomena in an experimental system, the width δd of the size distribution must satisfy the condition

$$\delta d / \langle d \rangle \ll \frac{1}{m}. \qquad (21)$$

The fractional thickness tolerance is more stringent for thicker slabs, so experimental tests of these predictions should ideally be conducted with frequencies that probe the lowest frequency ($m=1$) resonance of the slabs.

VIII. RELOCALIZATION TRANSITIONS

In Fig. 4 we plot reflectance versus angle of incidence on a slab of silica ($n=1.45$) embedded in air ($n=1$) and probed at various frequencies. Just as in the previous case, for frequencies below ω_c the reflectance minimum at normal incidence becomes smaller and smaller until the reflectance is zero for normal incidence when $\omega = \omega_c$. Above ω_c, likewise, the same delocalization phenomenon occurs, with the reflectance being zero at angles that increase with frequency.

Eventually, however, we reach a frequency (approximately $1.39\omega_c$ in this case) where the reflectance is nonzero for all angles. The reflectance remains nonzero for all angles until the frequency reaches $2\omega_c$, where the second transmission resonance becomes accessible (at normal incidence). At the frequency where the reflectance is nonzero for all angles we say that the wave is *relocalized*, because no transmission
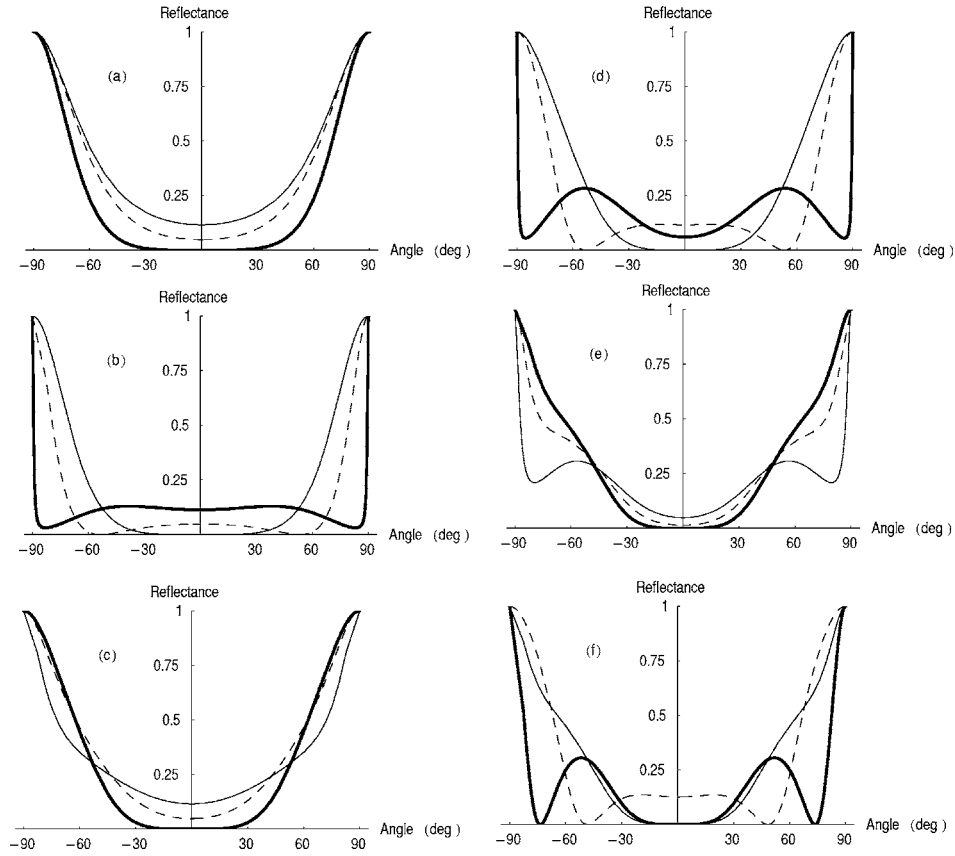
FIG. 4. Reflectance vs angle of incidence for a high index slab ($n=1.45$) embedded in a low index medium ($n=1$). (a) Approach to the first transmission resonance, with $\omega=0.6\omega_c$ (thin solid line), $0.8\omega_c$ (dashed), and ω_c (thick solid line). (b) The range of the first transmission resonance, with $\omega=\omega_c$ (thin solid line), $1.2\omega_c$ (dashed), and $1.39\omega_c$ (thick solid line). Notice that at $1.39\omega_c$ the reflectance is nonzero at all angles. (c) Approach to the second transmission resonance, with $\omega=1.6\omega_c$ (thin solid line), $1.8\omega_c$ (dashed), and $2\omega_c$ (thick solid line). (d) The range of the second transmission resonance, with $\omega=2\omega_c$ (thin solid line), $2.4\omega_c$ (dashed), and $2.77\omega_c$ (thick solid line). (e) Approach to the third transmission resonance, with $\omega=2.8\omega_c$ (thin solid line), $2.9\omega_c$ (dashed), and $3\omega_c$ (thick solid line). (f) Above the third transmission resonance, with $\omega=3\omega_c$ (thin solid line), $3.5\omega_c$ (dashed), and $4\omega_c$ (thick solid line).

resonance is accessible to allow power law transport over long distances. Instead, at large z the wave behavior is dominated by the (exponential) localized behavior of whichever channel has the longest localization length.

As we look at the plots of reflectance versus angle at higher frequencies in Fig. 4, we see that the reflectance again goes to zero for normal incidence at ω_c. For frequencies between $2\omega_c$ and $\approx 2.77\omega_c$ there is always an angle at which the reflectance is zero, until relocalization occurs at $\omega \approx 2.77\omega_c$. As at $2\omega_c$ there is another delocalization transition at $3\omega_c$, where the reflectance of the slab again goes to zero. At all frequencies above $3\omega_c$, however, there is always at least one angle at which the reflectance of the slab is zero, and the wave remains delocalized at all frequencies above $3\omega_c$. This sequence of delocalization and relocalization transitions is summarized in Fig. 5.

The occurrence of relocalization transitions is easy to understand. The resonance condition Eq. (4) requires that the z component of the wave vector (inside the slab) be an integer multiple of π/d. At $\omega=\omega_c$ the wave vector's magnitude is precisely π/d, so the resonance occurs for normal incidence. Above ω_c the wave vector's magnitude exceeds π/d and the resonance condition is satisfied for progressively larger

angles of incidence, the angle increasing to keep constant the z component of a progressively longer wave vector. In a slab with a lower index than its surroundings (e.g., an air gap surrounded by silica) the wave vector can point in any direction. In a high index slab surrounded by a low index medium (e.g., a silica slab in air), however, refraction always bends the wave vector toward the z axis, and the phenomenon of total internal reflection ensures that inside the slab the angle between the wave vector and the z axis will never exceed a certain upper bound. For sufficiently large frequencies the projection of the wave vector onto the z axis will always exceed π/d, regardless of the angle of incidence.

At some sufficiently high frequency there is always at least one angle of incidence that yields resonant transmission, due to the fact that the number of accessible transmission resonances increases linearly with frequency. This frequency corresponds to the final delocalization transition in our doped multilayer stack. How high this frequency is (and how many successive delocalization and relocalization transitions the system undergoes before reaching it) depends on the refractive index contrast between the slabs and the surrounding medium. It is straightforward to show that the final delocalization transition occurs at the mth transmission reso-
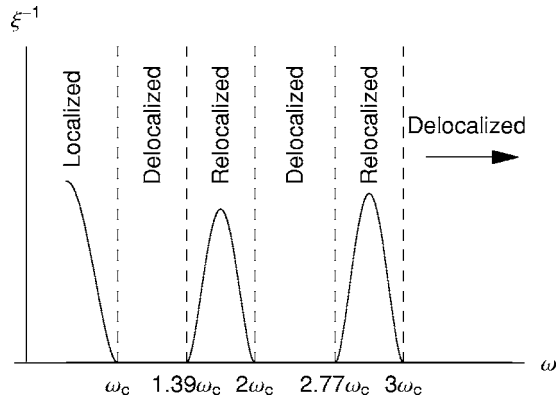
FIG. 5. Schematic depiction of the localized and delocalized bands of states in a system of high index (n=1.45) slabs in air (n=1) doped with weak 3D scatterers.

FIG. 6. Ensemble-averaged localization length ξ as a function of transverse wave vector. The straight line has slope −2, and an intercept chosen by averaging the first point in each of the data sets.

nance, where m is the smallest integer satisfying

$$m \geq \frac{\sqrt{1 - n_b^2/n^2}}{1 - \sqrt{1 - n_b^2/n^2}}. \tag{22}$$

For the case of silica in air, Eq. (22) predicts m=3, which is consistent with the calculations shown in Fig. 4. For higher contrast, such as silicon slabs surrounded by silica ($n/n_b \approx 3.5/1.5$ at λ=1.4 μm), Eq. (22) predicts (and calculations similar to those in Fig. 4 confirm) that m=10. Clearly, a large number of transmission windows may be achievable with common materials.

IX. COMPARISON WITH OTHER ANOMALOUS TRANSPORT PHENOMENA IN 1D DISORDERED SYSTEMS

The phenomenon described here is unique to the case of Fabry-Perot resonances and similar situations involving resonances of the constituent scatterers (e.g., slabs of random thickness, with antireflection coatings on each side). A similar effect would not occur in the more general case of transmission resonances created by multiple scattering and interference, since the angular width of those resonances decreases exponentially with sample thickness, rather than as a power law. In systems exhibiting a Brewster anomaly, it is clear that the frequency-dependent phenomena described here would not occur. However, further work is needed to determine whether similar delocalization phenomena could occur in such systems.

X. CONCLUSIONS

In conclusion, we have shown that waves can be delocalized by dopants that break translational symmetry along the transverse direction in a multilayer film that exhibits Fabry-Perot resonances. This effect occurs even for weakly scattering dopants, in stark contrast to previous predictions for waves in anisotropic disordered media. The delocalization transition occurs in a manner analogous to a second order phase transition. This rich behavior arises from resonances of the constituent layers, a phenomenon not described in other
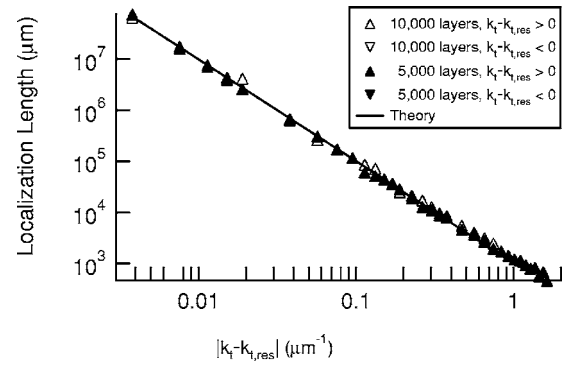
studies. This work therefore shows that the field of waves in anisotropic systems is richer than previously anticipated. Avenues for further work include more precise predictions of the exponent, and the question of whether analogous phenomena occur in electronic systems.

APPENDIX: SIMULATIONS OF MULTILAYER STACKS

We tested the predictions laid out in Sec. III B by calculating the transmittance of a multilayer stack as a function of sample thickness and angle of incidence θ. Our goal was to verify that the ensemble-averaged transmittance of the systems described in Sec. II scales with transverse wave vector in the manner predicted by Eq. (8).

For our numerical work, our systems were multilayer stacks of alternating silica slabs (n=1.45) of uniform thickness d, and air gaps (n_b=1) with random thicknesses. The thicknesses of the air gaps were uniformly distributed between d and $4d$. We considered illumination by light with a wavelength of 500 nm, and the slab thickness d=176.78 nm was chosen so that the Fabry-Perot resonance would occur for an arbitrarily chosen incident angle of θ=30° We studied systems with sizes ranging from 625 layers ($\approx$190 μm) to 10^4 layers ($\approx$3100 μm).

We performed our calculations using the 2×2 transfer matrix method for layered media [19]. All calculations were performed in MATHEMATICA. To test our code we verified that the reflectance of the slabs was zero for an incident angle θ=30°, and that the reflectance and transmittance added to unity with an accuracy of 1 part in 10^6 or greater. When calculating ensemble averages we randomly generated 100 systems with the parameters described in the previous paragraph. From the ensemble-averaged transmittance we calculated a localization length using the relation $T=e^{-2L/\xi(\omega,k_t)}$.

In Fig. 6 we show the ensemble-averaged results for the localization length as a function of direction. The range of transverse wave vectors considered corresponds to an angu-
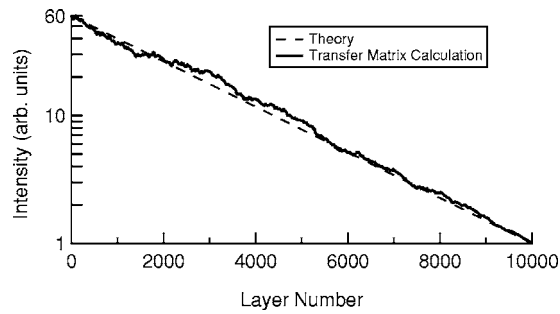
FIG. 7. Intensity vs layer number inside a random medium excited at an angle of incidence $\theta = 26°$, averaged over 100 different random systems with the same thickness ($L = 3100$ μm) and volume fraction of scatterers. The straight line is an exponential (predicted by theory) with the appropriate incident and transmitted intensities.

lar width of approximately 5°. We show results from systems with 5×10^3 and 10^4 layers to verify that our predictions are not dependent on our choice of system size. The dashed line in the log-log plot has slope -2, corresponding to a power law with the theoretically predicted exponent -2 from Eq. (8). For both system sizes we see that the computational results agree well with the predictions of Eq. (8).

As a test of our simulations, we also verified that that the ensemble-averaged intensity decays exponentially inside our system. In Fig. 7 we show the wave intensity as a function of position inside our system, averaged over 100 different configurations. The log-linear plot clearly shows that the ensemble-averaged intensity decays exponentially as a function of position, as predicted by theory.

We also demonstrate explicitly that our results are *only* valid for ensemble averages rather than single systems. In Fig. 8 we show calculations of the localization length $\xi(\omega, k_t)$ as a function of transverse wave vector k_t for two systems of different thicknesses. (ξ is normalized to the sample thickness for convenience.) In both cases we see that for k_t very close to $k_{t,res}$ (i.e., very close to a Fabry-Perot resonance) the localization length $\xi(\omega, k_t)$ scales as predicted. However,
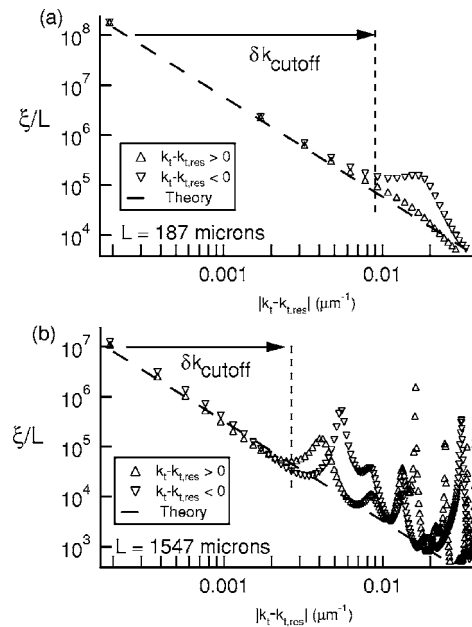
FIG. 8. Localization length ξ as a function of transverse wave vector. The straight lines have slope -2, and the intercept is the average of the first data point in each of the data sets. (a) System of 625 slabs (187 μm) thick; (b) system of 5000 slabs (1547 μm thick).

there is a detuning δk_{cutoff} past which $\xi(\omega, k_t)$ fluctuates as a function of k_t. Our investigations show that the cutoff varies from sample to sample. The trend is that the average value of δk_{cutoff} decreases with increasing sample thickness, but we have not found a systematic dependence on sample thickness.

These numerical results imply that our results in Sec. III B are valid when averaged over ensembles of similar systems. Within a single system our results are only valid for transport in directions very close to a Fabry-Perot resonance.

[1] P. W. Anderson, Phys. Rev. **109**, 1492 (1958).
[2] P. W. Anderson, Philos. Mag. B **52**, 505 (1985).
[3] S. John, Phys. Rev. Lett. **58**, 2486 (1987).
[4] D. S. Wiersma, P. Bartolini, A. Lagendijk, and R. Righini, Nature (London) **390**, 671 (1997).
[5] E. Yablonovitch, Phys. Rev. Lett. **58**, 2059 (1987).
[6] P. M. Johnson, B. P. J. Bret, J. G. Rivas, J. J. Kelly, and A. Lagendijk, Phys. Rev. Lett. **89**, 243901 (2002).
[7] R. Sapienza, S. Mujumdar, C. Cheung, A. G. Yodh, and D. Wiersma, Phys. Rev. Lett. **92**, 033903 (2004).
[8] W. Xue, P. Sheng, Q. J. Chu, and Z. Q. Zhang, Phys. Rev. Lett. **63**, 2837 (1989).
[9] Z. Q. Zhang, Q. J. Chu, W. Xue, and P. Sheng, Phys. Rev. B **42**, 4613 (1990).
[10] P. Sheng and Z. Q. Zhang, Phys. Rev. Lett. **74**, 1343 (1995).
[11] P. Sheng, *Introduction to Wave Scattering, Localization, and Mesoscopic Phenomena* (Academic, San Diego, 1995).
[12] K. Y. Bliokh, Y. P. Bliokh, and V. D. Freilikher, J. Opt. Soc. Am. B **21**, 113 (2004).
[13] J. Bertolotti, S. Gottardo, D. S. Wiersma, M. Ghulinyan, and L. Pavesi, Phys. Rev. Lett. **94**, 113903 (2005).
[14] X. Du, D. X. Zhang, X. L. Zhang, B. H. Feng, and D. Z. Zhang, Phys. Rev. B **56**, 28 (1997).
[15] J. E. Sipe, P. Sheng, B. S. White, and M. H. Cohen, Phys. Rev. Lett. **60**, 108 (1988).
[16] M. Born and E. Wolf, *Principles of Optics: Electromagnetic Theory of Propagation, Interference and Diffraction of Light* (Cambridge University Press, Cambridge, England, 1999).
[17] F. Qiu, R. W. Peng, X. Q. Huang, Y. M. Liu, M. Wang, A. Hu, and S. S. Jiang, Europhys. Lett. **63**, 853 (2003).
[18] T. Hattori, N. Tsurumachi, S. Kawato, and H. Nakatsuka, Phys. Rev. B **50**, 4220 (1994).
[19] P. Yeh, *Optical Waves in Layered Media* (Wiley, New York, 1988).